ELSEVIER

Chemical Engineering Journal 133 (2007) 273–281

Chemical Engineering Journal

www.elsevier.com/locate/cej

Sorptive response profile of an adsorbent in the defluoridation of drinking water

S. Ayoob, A.K. Gupta *

Environmental Engineering Division, Department of Civil Engineering, Indian Institute of Technology, Kharagpur 721 302, India

Received 13 December 2006; received in revised form 15 February 2007; accepted 21 February 2007

Abstract

The presence of excess fluoride in drinking water has become a potential cause of agony to hundreds of million people the world over as it initiates the debilitating disease fluorosis. This concern imparts enough impetus among the water community for concerted research on defluoridation of drinking water. The present study evaluates the feasibility of using an adsorbent, alumina cement granules (ALC) in removing fluoride from water through batch and column studies. In batch studies, it was observed that a dose of 2 g l^{-1} of ALC could bring down fluoride concentrations in water from 8.65 mg l^{-1} to below the permissible level of 1.0 mg l^{-1} at optimum conditions. The equilibrium sorption data, generated by dose variations of ALC, were better modeled by Freundlich isotherm. The maximum monolayer capacity of ALC suggested by the Langmuir model was 10.215 mg g^{-1}. In column studies, the maximum adsorption capacity of ALC at the point of breakthrough was found to be 2.27 mg g^{-1} at a flow rate of 4 ml min^{-1}. The responses of the adsorbent in the fixed bed for varying operating conditions of bed depth, flow rate, and initial fluoride concentrations were analyzed. The sorption kinetic models; Hutchins BDST, Thomas, Yoon–Nelson, and Clark were examined to describe the sorption process. The characteristic parameters of the respective models for the process design of columns were obtained by their linear regression. Among all the models tested, the Clark's model could better describe the sorption process at all sorptive conditions and ranges analyzed. The study also suggested the use of sorption contours of effluent fluoride concentration for better visual evaluation and correlation of experimental sorption profiles with the model. The sorption contours could aid in the quantitative evaluation of service times of columns at various stages of breakthrough for any bed depth, flow rate and initial fluoride concentration within the ranges studied.

Keywords: Adsorption; Breakthrough curve; Column study; Fluoride; Modeling

1. Introduction

Water, revered as our culture and life, has many homes in human habitat. Nonetheless, the Millennium Development Goal of safe drinking water is still a dream for about 1.1 billion people in the developing world [1]. Of late, this dwindling availability of fresh water and its increasing pollution from diverse sources raises overarching global concerns. Further, the entry of geogenic pollutants like fluoride in drinking water sources takes this growing global water crisis to ominous dimensions. Fluorosis, resulting from intake of excess fluoride, has struck more than 25 countries of the world. In India alone, the lives of more than 66 million people including 6 million children are 'at risk' of fluorosis [2]. In China, over 26 million people suffer from dental fluorosis [3], and 10 million from skeletal fluorosis [4]. The notion of this human vulnerability to excess fluoride in drinking water obsessed with its well-documented legitimate concerns [5] catalyzes global defluoridation research.

Though many technologies like coagulation, adsorption and/or ion exchange, electrochemical methods and applications of membranes are suggested for defluoridation, a lasting solution is still at large. Coagulation methods are generally effective in defluoridation, but are unsuccessful in bringing fluoride to the desired concentration levels. The electrochemical techniques in general, suffer due to high cost factor, both during installation and maintenance. Membrane separations can be performed at low temperatures under isothermal conditions leading to low energy consumption. But they are relatively expensive to install and operate and are prone to fouling, scaling, or membrane degradation. Especially for developing countries, the high cost of these technologies may be a major constraint for imple-

* Corresponding author. Tel.: +91 3222 283428; fax: +91 3222 282254.
E-mail addresses: ayoobtkm@yahoo.co.in (S. Ayoob), akgupta@iitkgp.ac.in (A.K. Gupta).

1385-8947/$ – see front matter © 2007 Elsevier B.V. All rights reserved.
doi:10.1016/j.cej.2007.02.013

Nomenclature

A, r	Clark constants
b	Langmuir constant related to binding energy or affinity parameter
bt	time for breakthrough (h)
C	constant related to thickness of the boundary layer (mg g^{-1})
C_{ad}	adsorbed fluoride concentration in the fixed bed (mg l^{-1})
C_e	concentration of fluoride in the solution at equilibrium (mg l^{-1})
C_t	concentration of fluoride in the solution at any time t (mg l^{-1})
$C_{t(exp)}$	effluent fluoride concentration from the column (mg l^{-1})
$C_{t(theo)}$	effluent fluoride concentration predicted by the model (mg l^{-1})
C_0	initial concentration of fluoride in solution (mg l^{-1})
et	time for exhaust (h)
EBCT	empty bed contact time (min)
F_b	quantity of fluoride sorbed onto ALC in the column up to breakthrough (mg)
F_{tot}	quantity of fluoride sorbed onto ALC in the column up to exhaust (mg)
k_p	intraparticle diffusion rate constant (mg g^{-1} h$^{-1/2}$)
k_{Th}	Thomas rate constant (l h^{-1} mg^{-1})
k_{YN}	rate constant of Yoon and Nelson equation (h^{-1})
K	adsorption rate constant (l mg^{-1} h^{-1})
K_f	Freundlich constant representing adsorption capacity (l g^{-1})
m	mass of ALC used in batch study (g)
N	number of samplings
N_0	adsorption capacity of the adsorbent (mg l^{-1})
q_{col}	total adsorption capacity of ALC in the fixed bed (mg g^{-1})
q_e	amount of fluoride sorbed onto ALC at equilibrium (mg g^{-1})
q_{max}	Langmuir constant related to saturated monolayer adsorption (mg g^{-1})
$q_{min,col}$	minimum adsorption capacity of ALC in fixed the bed (mg g^{-1})
q_t	amount of fluoride sorbed onto ALC at any time t (mg g^{-1})
q_{Th}	equilibrium sorbent uptake of the adsorbent predicted by Thomas model (mg g^{-1})
Q	volumetric flow rate (l h^{-1})
t	service (sampling) time of the fixed bed (h)
t_{50}	service time of the fixed bed corresponding to 50% breakthrough (h)
u	linear flow velocity of feed to bed (cm h^{-1})
V	volume of fluoride solution (l)
V_b	volume of water treated up to breakthrough (l)
V_e	volume of water treated up to exhaust (l)
Z	fixed bed depth of adsorbent in the column (cm)
$1/n$	Freundlich constant representing adsorption intensity

Greek symbol

τ	time required for 50% adsorbate breakthrough (h)

mentation. Among the options, adsorption has been regarded as a promising technology practiced in many fluoride endemic areas of the developing world. The use of adsorbents in sorptive filtration system assures a number of process engineering advantages like simplicity in operations, high yield in purification process, automation in treatment protocol and above all, easy scaling-up from laboratory to field. The pollutants in water are removed by getting concentrated onto a small adsorbent mass, which can eventually be regenerated or disposed off [6,7]. In this direction, the successful use of activated alumina for fluoride removal and its effective implementations are well documented [8–10]. However, issues like need for more contact time for desired removal due to its slow kinetics, low pH range for optimum removal necessitating pre-treatment, turns disadvantageous.

It has been observed that most of the reported defluoridation research is confined to batch studies, which only suggest the feasibility of an adsorbent for sorption and renders its adsorption capacity through best-fitting isotherms and some kinetic models. However, the actual capacity of the adsorbent in fixed bed column studies, which dictates its field defluoridation potential, is rarely reported. The capacity of an adsorbent for field use and its features of removal can be totally evaluated only by analyzing its sorptive responses both in batch and column studies. These responses can be described and compared by modeling the system for scaling-up. In the process of modeling, though the unsteady situation prevailing in fixed bed poses difficulties [7], it is desirable to use simplified model expressions to describe the sorptive responses, as demonstrated in many recent sorption studies [11,12].

This paper researches into the feasibility of using an adsorbent, alumina cement granules (ALC), in defluoridating drinking water by analyzing the effect of various factors affecting its sorption profile. The objective is to focus on to evaluate, describe and predict its dynamic sorptive responses from batch and column studies through modeling.

2. Materials and methods

2.1. Adsorbate and chemicals

All chemicals and reagents used in this study were of analytical grade. NaF (Merck) was used for preparation of standard fluoride stock solution in double distilled water. All synthetic fluoride solutions for adsorption and analysis were prepared by appropriate dilution of the stock solution in de-ionized (DI)

water. Only plastic wares were used for handling fluoride solution and it is not prepared in or added to glass containers. All plastic wares were washed in dilute HNO_3 acid bath and rinsed thoroughly with DI water prior to use.

2.2. Analysis

Expandable ionAnalyzer EA 940 with Orion ionplus (96-09) fluoride electrode (Thermo Electron Corporation, USA), using TISAB III buffer was used for fluoride measurement. The pH measurement was done by a Cyber Scan 510 pH meter (Oakton Instruments, USA). A temperature controlled orbital shaker (Remi Instruments Ltd., Mumbai, India) was used for agitation of the samples in batch studies. A high precision electrical balance (Mettler Toledo, Model AG135) was used for weight measurement. The elemental composition of ALC combined with oxygen was determined by Energy Dispersive X-ray (EDX) analysis (Oxford ISIS-300 model) by quantitative method in two iterations using ZAF correction, at a system resolution of 65 eV, and results were normalized stoichiometrically.

2.3. Synthesis of the adsorbent

The adsorbent ALC, selected for the present research, was prepared from commercially available high alumina cement. The high proportion of alumina and calcium, whose (established) potential in fluoride removal was instrumental in selection. Initially, a slurry was prepared by adding distilled water to 1 kg of high alumina cement at a water–cement ratio of ~0.3. The slurry was kept at ambient temperature for 2 days for setting, drying and hardening. This hardened paste was cured in water for 5 days. After curing, it was broken, granulated, sieved to geometric mean size of ~0.212 mm, and kept in airtight containers for use. The elemental composition of ALC (combined with oxygen) obtained from EDX showed proportions of Al_2O_3 (78.49%), CaO (15.82%), SiO_2 (5.39%), and Fe_2O_3 (0.30%). The bulk density, specific gravity and pH of zero point charge (pHzpc) were 2.33 g cm^{-3}, 2.587 and 11.32, respectively. The pH at zero point charge of ALC was determined as per the method suggested by Noh and Schwarz [13]. Different quantities of ALC were placed in 10 ml solutions of 0.1 M NaCl (prepared in preboiled water) in various bottles and kept in the thermostat shaker for overnight continuous agitation. The equilibrium pH values of these mixtures were measured and limiting value was reported as pHzpc of ALC.

2.4. Batch and column studies

The feasibility of ALC in fluoride removal was evaluated through its kinetic and equilibrium adsorption responses under completely mixed batch reactor (CMBR) technique commonly known as batch studies. Polyethylene bottles (Tarson Co. Ltd., India) of 150 ml capacity with 50 ml of synthetic fluoride solutions in DI water were used in these investigations. ALC was added as per dose requirements to these bottles and were shaken in an orbital shaking incubator at 230 ± 10 rpm. Equilibrium studies were carried out with ALC dose range of 1–3 g l^{-1} and kinetic studies at a fixed dose of 2 g l^{-1} for an initial fluoride concentration of 8.65 mg l^{-1}. The bottles were taken out after 3 h of agitation and content was filtered using Whatman No-42 filter paper to separate the sorbent and filtrate. From the filtered sample of each batch reactor, 10 ml was taken for analysis and determination of residual fluoride. All experiments were duplicated and average values were used for further calculations. In order to check for any adsorption on the walls of the container, blank container adsorption tests were carried out.

The applicability of ALC for field use was evaluated through continuous flow fixed bed column experiments using glass columns of length 550 mm and internal diameter 20 mm. The column was packed with desired depth of ALC between two layers of glass wool at the top and bottom ends to prevent the absorbent from floating. Then the column was fed continuously with fluoride water at desired volumetric flow rate using peristaltic pumps (Miclins, India). The effluent samples were collected at pre-determined time intervals and analyzed for remaining fluoride concentration. All studies were performed at a constant temperature of 300 K, representative of the prevailing environmental conditions.

2.5. Adsorption capacity of ALC

In batch studies, the experimental adsorption capacity of ALC was calculated as

$$q_t = \frac{C_0 - C_t}{m} V \tag{1}$$

In column studies, the total quantity of fluoride adsorbed in the column for a given feed concentration and flow rate could be found by calculating the area above breakthrough curve by integrating the adsorbed fluoride concentration versus time t (h) plot as

$$F_{\text{tot}} = Q \int_{t=0}^{t=\text{et}} C_{\text{ad}}\, \text{d}t \tag{2}$$

similarly, the quantity of fluoride adsorbed up to breakthrough as

$$F_{\text{b}} = Q \int_{t=0}^{t=\text{bt}} C_{\text{ad}}\, \text{d}t \tag{3}$$

where

$$C_{\text{ad}} = C_0 - C_t \tag{4}$$

The fluoride removal capacity of column up to the point of breakthrough will be representing the 'breakthrough capacity', indicative of the column adsorption capacity in single column operation ($q_{\text{min,col}}$). This value obtained by dividing F_{b} by the mass of ALC in the column, turns useful in the design of domestic defluoridation units (DDU) which normally involve single chamber applications. Whereas, in series column operations, all columns except the last can be run up to the point of exhaust as these columns still contains unused adsorbents. In such cases, capacity up to exhaust will be its total or maximum capacity (q_{col}). This value obtained by dividing F_{tot} by the mass of ALC

in the column, will be appropriate and useful for field scale community applications involving number of columns.

2.6. Analysis and modeling of breakthrough profile

For a given bed depth, the service times of a continuous flow fixed bed unit (unit plant) are correlated with the initial sorbate concentration, flow rate, and adsorption capacity of the adsorbent used. So, obtaining a reliable adsorption capacity of the adsorbent, and describing the sorptive responses of the fixed bed, turns crucial in efficient process design and operation. This necessitates a careful evaluation and analysis of the experimental data, to predict the effect of variations in operational parameters of sorption process for optimum performance, through modeling. The models selected to describe the sorption of fluoride on ALC include Hutchins BDST model [14], Thomas model [15], Yoon–Nelson model [16], and Clark's model [17]. The assumptions involved in the derivations of these models with their respective linear forms are shown in Table 1.

In all cases, the average percentage errors (APE) between the experimental and predicted values of effluent concentrations were calculated as

$$\mathrm{APE}\% = \frac{\sum_{t=1}^{N} |(C_{t(\mathrm{exp})} - C_{t(\mathrm{theo})})/C_{t(\mathrm{exp})}|}{N} \times 100 \quad (5)$$

3. Results and discussion

3.1. Batch adsorption studies

The kinetic curve of fluoride sorption by ALC is shown in Fig. 1. The uptake is characterized by a rapid phase at the initial few minutes followed by a slow phase. Around 70% removal of fluoride takes place within the first 10 min itself. The removal is stabilizing after 150 min with negligible removal after 3 h implying attainment of equilibrium. The initial rapid uptake may indicate a surface bound sorption [18] and precipitative removal; whereas, the slow and gradual uptake in the second phase may be due to long-range diffusion of fluoride ions into interior pores of ALC. This biphasic uptake demonstrates the key role of mass transfer in the removal process [19].

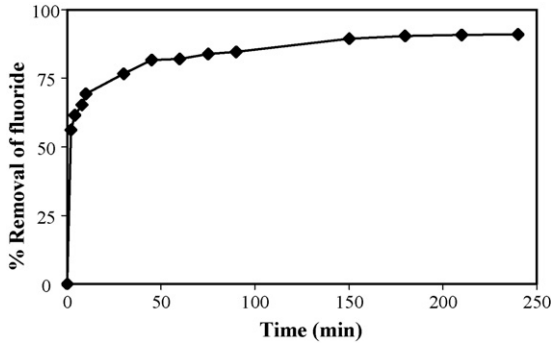

Fig. 1. The kinetic curve of adsorption of fluoride onto ALC ($C_0 = 8.65\,\mathrm{mg\,l^{-1}}$, dose of ALC = $2.0\,\mathrm{g\,l^{-1}}$, pH 6.9 ± 0.4).

Generally three consecutive steps, namely bulk diffusion, film diffusion and pore diffusion are involved in the adsorption of materials from solution by porous adsorbents [20]. In general, pore diffusion is the rate-limiting step in batch systems which provide a high degree of agitation. Many recent studies involving adsorption of fluoride on metal oxides established intraparticle surface diffusion as rate limiting [21,22]. The possibility of intraparticle diffusion in the sorption of fluoride onto

Table 1
The linear form of the sorption models with their characteristic features

Model	Characteristic features	Linear form	Plot
Hutchins BDST model	Derived based on the assumptions that intraparticular diffusion and external mass resistance are negligible and that the adsorption kinetics is controlled by surface chemical reaction between solute in the solution and the unused adsorbent	$t = aZ + b$, where $a = \frac{N_0}{C_0 u}$, $b = -\frac{1}{KC_0} \ln\left[\frac{C_0}{C_t} - 1\right]$	t vs. Z
	The BDST model also serves as a useful tool for comparing the performance of columns operating under different process variables	If C_0 changes to a new value C_1, constants a' and b' will be: $a' = a\left(\frac{C_0}{C_1}\right)$, $b' = b\left(\frac{C_0}{C_1}\right)\frac{\ln(C_1/C_t - 1)}{\ln(C_0/C_t - 1)}$ If u changes to u', the new gradient a' will be: $a' = a\left(\frac{u}{u'}\right)$ At 50% breakthrough, $t_{50} = aZ$	
Thomas model	Derived by assuming Langmuir kinetics of adsorption–desorption with no axial dispersion and that the rate driving force obeys second-order reversible reaction kinetics	$\ln\left(\frac{C_0}{C_t} - 1\right) = \frac{k_{\mathrm{Th}} q_{\mathrm{Th}} M}{Q} - k_{\mathrm{Th}} C_0 t$	$\ln[(C_0/C_t) - 1]$ vs. t
Yoon–Nelson model	Derived based on the assumption that the rate of decrease in the probability of adsorption for each adsorbate molecule is proportional to the probability of adsorbate adsorption and the probability of adsorbate breakthrough on the adsorbent	$\ln\left(\frac{C_t}{C_0 - C_t}\right) = k_{\mathrm{YN}} t - \tau k_{\mathrm{YN}}$	$\ln[C_t/(C_0 - C_t)]$ vs. t
Clark model	Derived based on the use of mass-transfer concept in combination with Freundlich isotherm	$\ln\left(\left[\frac{C_0}{C_t}\right]^{n-1} - 1\right) = \ln A - rt$	$\ln[(C_0/C_t)^{n-1} - 1]$ vs. t

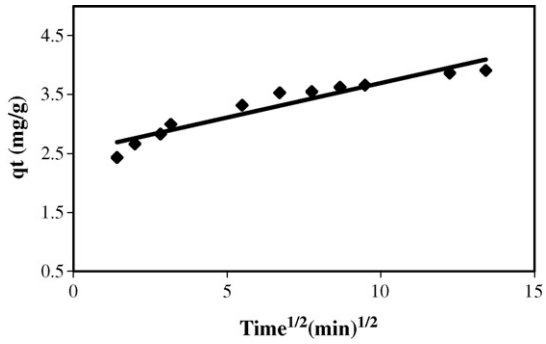

Fig. 2. The linear intraparticle diffusion plot of fluoride sorption on ALC (C_0 = 8.65 mg l^{-1}, dose of ALC = 2.0 g l^{-1}, pH 6.9 ± 0.4).

ALC is explored using Eq. (6) by plotting the fluoride uptake (q_t) against square root of time ($t^{1/2}$) [23] as:

$$q_t = k_p t^{1/2} + C \quad (6)$$

The value C gives an idea about thickness of the boundary layer (larger the value, greater is the boundary effect). According to this model, the plot q_t versus $t^{1/2}$ should be linear if intraparticle diffusion is involved in the adsorption system and if it passes through the origin, intraparticle diffusion is the rate-controlling step. As shown in Fig. 2, the plot of q versus $t^{1/2}$ gives a straight line (R^2 = 0.912), indicating the significance of intraparticle diffusion in the sorption process. The values of k_p and C are 0.117 mg g^{-1} h$^{-1/2}$ and 2.526 mg g^{-1}, respectively. As the line does not pass through origin, it can be surmised that intraparticle diffusion is not the only rate-limiting step, but other kinetic factors may also control the rate of adsorption, in addition to some degree of boundary layer control [24,25] as indicated by C value. This observation, together with biphasic nature of the sorption kinetics further suggests that, fluoride removal by ALC is complex with more than one mechanism limiting the rate of sorption. It appears that the surface heterogeneity of ALC, or reactions other than surface complexation of fluoride with metal oxides, may influence the overall sorption process.

The adsorption capacity analysis was done by Langmuir and Freundlich isotherms represented by Eqs. (7) and (8), respectively [26,27], and their correlations with experimental data points are shown in Fig. 3:

$$q_e = \frac{q_{max} b C_e}{1 + b C_e} \quad (7)$$

$$q_e = k_f C_e^{1/N} \quad (8)$$

In linear regression of the above two models, Freundlich isotherm showed better correlation (R^2 = 0.973) with experimental equilibrium data (generated by dose variations of ALC) than Langmuir (R^2 = 0.959). The Freundlich constants K_f and $1/n$ were 5.192 and 0.595, respectively. The model rendered the maximum Langmuir monolayer capacity of ALC (q_{max}) as 10.215 mg g^{-1}.

3.2. Effect of process parameters on breakthrough profile

The breakthrough curves obtained by varying the depths of ALC bed, flow rates and initial fluoride concentrations are presented in Fig. 4. The respective service times, volumes of water treated, and the adsorption capacity of the columns under various process conditions are illustrated in Table 2. A closer examination of the breakthrough curves, especially at lower C_t/C_0 ranges, indicates that the curves turns less steeper at higher bed depths under same flow rates. Also, both breakthrough and exhaust times increase with corresponding volumes of water treated, with increase in bed depths. It is naturally expected that the availability of more adsorbent at higher bed depths offer more surface area and binding sites for sorption resulting enlarged mass-transfer zones. The adsorption capacity of ALC at different bed depths (5–15 cm) for a particular flow rate (8 ml min^{-1}) shows only marginal variation, indicating its consistency in and affinity for fluoride sorption. However, the observed reduction in total adsorption capacity at higher bed depths are unexpected which may be due to some localized channelization or uneven flow patterns developed in the bed after breakthrough.

The breakthrough curves developed for the same bed height (10 cm) at higher flow rates appeared steeper which may be due to faster movement of adsorption zone along the bed. The breakthrough capacity of the column ($q_{min,col}$) showed consistent increase, though marginal, with reduction in flow rates. This behavior is normally expected due to better diffusivity of fluoride resulting in enhanced sorption at higher empty bed contact times (EBCT = volume of ALC bed/volumetric flow rate). The kinetic

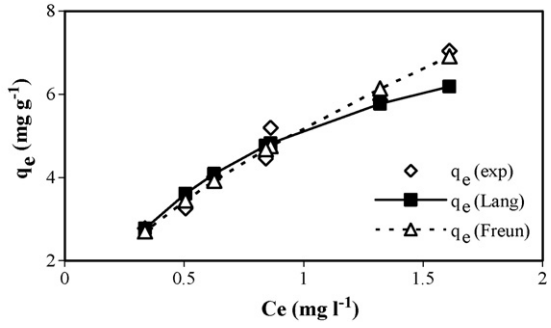

Fig. 3. Correlations of Langmuir and Freundlich isotherm models with the experimental data (C_0 = 8.65 mg l^{-1}, dose of ALC = 1–3 g l^{-1}, pH 6.9 ± 0.4).

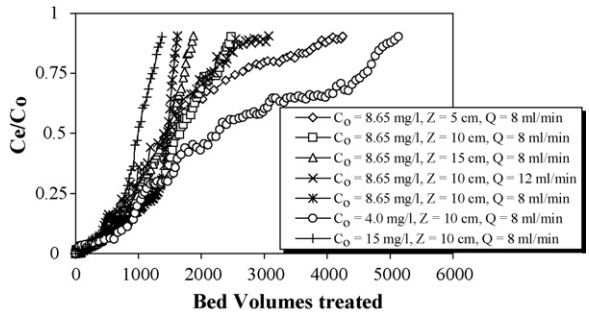

Fig. 4. Experimental breakthrough curves of fluoride sorption onto ALC with bed volumes of water treated at different bed depths, flow rates and initial fluoride concentrations.

Table 2
Adsorption data for fixed bed of ALC for fluoride sorption at different process conditions

Initial fluoride concentration, C_0 (mg l^{-1})	ALC bed depth, Z (cm)	Flow rate, Q (ml min^{-1})	EBCT (min)	Time for breakthrough, bt (h)	Volume of water treated up to point of breakthrough, V_b (l)	Bed volumes up to point of breakthrough	$q_{min,col}$ (mg/g)	Time for exhaust, et (h)	Volume of water treated up to exhaust, V_e (l)	Bed volumes up to exhaust	q_{col} (mg/g)
8.65	5	8	4.575	17	8.16	519.48	1.846	139	66.72	4247.54	6.965
8.65	10	8	9.149	33	15.84	504.20	1.802	162	77.76	2475.18	5.849
8.65	15	8	13.724	58	27.84	590.78	2.096	184	88.32	1874.21	4.875
8.65	10	4	18.299	84	20.16	641.71	2.270	212	50.88	1619.56	4.841
8.65	10	12	6.099	20	14.40	458.37	1.635	134	96.48	3071.06	5.616
4.00	10	8	9.149	72	34.56	1100.08	1.722	336	161.28	5133.71	4.594
15.0	10	8	9.149	22	10.56	336.14	2.087	90	43.20	1375.10	6.163

curve (Fig. 1) also shows identical response in the EBCT ranges corresponding to the flow rates. So, it appears that batch and column studies follow similar trends of sorption. It is observed that the volumes of water treated at breakthrough and exhaust reduces considerably with increase in initial concentrations of fluoride from 4 to 15 mg l^{-1}. Also the service times of column indicates that high fluoride concentrations aids quick saturation of the bed and faster movement of adsorption zone. As the higher concentration gradient between the solute in solution and solute on the sorbent results in enhanced diffusion and sorption, the adsorption capacity of ALC is also found increasing (Table 2) at higher initial fluoride concentrations. The range of EBCT provided (~4.5–18.3 min) in this study ensures around 75–80% of the total removal observed in batch system represented by the kinetic curve (Fig. 1). The column performance of ALC renders average adsorption potential of 5.896 mg g^{-1} at the point of exhaust, whereas, batch studies suggests a much higher value of 10.215 mg g^{-1} as its maximum Langmuir monolayer adsorption capacity. Theoretically, the adsorption capacities from batch studies may not give accurate scale up information about column operation system [28]. This is mainly because the adsorption media has not been subjected to equilibrium sorption thereby not getting totally exhausted in columns as in batch system. Also, uneven flow patterns throughout the column may results in incomplete exhaustion of bed as cited earlier.

3.3. Application of sorption models

In general, the characteristic parameters of the models obtained by linear regression were used to predict effluent fluoride concentrations. In the BDST model applications, the values of maximum adsorption capacity parameter N_0 (Table 3) is found decreasing with increasing bed depths, indicating that the adsorption zone is not moving with a constant speed along the column. The adsorption rate constants (K), characterizing the rate of solute transfer from liquid to solid phase, were observed increasing with flow rate and initial fluoride concentrations, indicating the influence of external mass transfer on system kinetics. The higher values of K are advantageous as it indicates that even a short bed will avoid breakthrough. Theoretically, the slope of BDST line represents time required for adsorption zone to travel a unit length through adsorbent bed. In the present study, for 10 cm bed this value is calculated as 8.5, 4.25 and 2.833 h for 4, 8 and 12 ml min^{-1}, respectively. Thus predicted breakthrough times for 4 and 12 ml min^{-1} are obtained as 80 and 23.33 h, respectively, with corresponding exhaust times of 202.33 and 145.66 h. The time required for adsorption zone to travel a unit length through the 10 cm adsorbent bed are calculated as 9.191, 4.25 and 2.4508 h for initial fluoride concentrations of 4, 8.65 and 15 mg l^{-1}, respectively. The predicted breakthrough times for 4 and 15 mg l^{-1} are obtained as 86.072 and 20.981 h, respectively, with corresponding exhaust times of 345.626 and 92.168 h. A comparison of these predicted service times, with the experimental service times from Table 2, indicates that the model fails to predict service times in most of the cases. The predicted service times are found to be more than the corresponding experimental values. In the current study the t_{50} values

Table 3
The characteristic parameters predicted by BDST model, Thomas model and Yoon–Nelson model

Initial fluoride concentration ($mg\,l^{-1}$)	Bed depth (cm)	Flow rate ($ml\,min^{-1}$)	BDST model				Thomas model			Yoon–Nelson model					
			K ($l\,mg^{-1}\,h^{-1}$)	N_0 ($mg\,l^{-1}$)	R^2	APE	K_{Th} ($l\,mg^{-1}\,h^{-1}$)	q_0 ($mg\,g^{-1}$)	q_{Th} ($mg\,g^{-1}$)	R^2	APE	K_{YN} (h^{-1})	τ (h)	τ_{cal} (h)	R^2	APE
8.65	5	8	0.0048	08573.56	0.905	38.853	0.0048	6.965	7.970	0.905	38.853	0.0417	50.24	70.25	0.905	38.853
8.65	10	8	0.0039	14109.11	0.959	22.356	0.0039	5.849	6.048	0.959	22.356	0.0345	108.54	106.63	0.959	22.356
8.65	15	8	0.0035	11794.47	0.961	17.474	0.0035	4.875	5.062	0.961	17.474	0.0309	146.78	133.86	0.961	17.474
8.65	10	4	0.0025	12574.39	0.892	22.057	0.0025	4.841	5.396	0.892	22.057	0.0217	191.72	190.29	0.892	22.057
8.65	10	12	0.0048	13653.96	0.952	20.486	0.0049	5.616	5.859	0.952	20.486	0.0423	64.33	68.87	0.952	20.486
4.00	10	8	0.0032	11039.11	0.879	27.440	0.0032	4.594	4.738	0.879	27.440	0.0129	148.00	180.63	0.879	27.440
15.0	10	8	0.0045	14760.46	0.978	16.389	0.0046	6.163	6.335	0.978	16.389	0.0684	65.20	64.40	0.978	16.389

for 5, 10 and 15 cm bed depths are 50.24, 108.45 and 146.78 h, respectively. The plot of Z versus t_{50} offers a straight line plot ($R^2 = 0.985$) but quite deviates from the origin, indicating its inability to follow the model. Generally, this failure is attributed to the complexity of sorption process. So, it is rational to believe that intraparticle diffusion and external mass resistance do play an important role in the sorptive removal of fluoride by ALC in the column and that the kinetics are not controlled by the surface chemical reactions alone. This further supports the complexity of the sorption process suggested by the intraparticle diffusion model.

The linear regression of the Thomas model with the experimental fluoride sorption data also shows reasonably good correlations in most of the cases (Table 3). The values of K_{Th} are found increasing with increase in flow rates and initial fluoride concentrations. As shown, both the parameters q_{Th} and K_{Th} of the model are found decreasing with higher bed depths. For all conditions of bed depths, flow rates and initial fluoride concentrations, the model predicted marginally higher sorption capacity (q_{Th}) than experimental (q_0) values. As illustrated in Table 3, the rate constant of the Yoon–Nelson model (K_{YN}) decreased with increase in bed depths; but increases with flow rates and initial fluoride concentrations. From the experimental results and data regression, the model proposed by Yoon–Nelson provided a good correlation of sorption of fluoride by ALC in most of the cases. As demonstrated in batch studies the fluoride sorption by ALC follows Freundlich isotherm model, and its constant n is used for evaluating the parameters in Clark model. The model renders good fit with comparatively higher R^2 and lower APE values in most of the experimental conditions (Table 4). The value of r is observed increasing with flow rates and initial fluoride concentrations but decreases with bed depths.

3.4. Comparison of applied models

The adsorption models analyzed and experimented in this study to fit the fluoride sorption data can be essentially grouped based on their axial settings. In general, the linear fittings of Hutchins BDST, Thomas and Yoon–Nelson models can be represented as

$$\ln\left(\frac{C_0}{C_t} - 1\right) = k_1 - k_2 t \tag{9}$$

Table 4
The characteristic parameters predicted by Clark's model

Initial fluoride concentration ($mg\,l^{-1}$)	Bed depth (cm)	Flow rate ($ml\,min^{-1}$)	Clark's model			
			$\ln A$	r (h^{-1})	R^2	APE
8.65	5	8	1.927	0.0362	0.929	35.783
8.65	10	8	2.523	0.0289	0.970	20.045
8.65	15	8	2.913	0.0258	0.963	15.676
8.65	10	4	2.873	0.0177	0.862	22.736
8.65	10	12	1.986	0.0374	0.969	17.140
4.00	10	8	1.481	0.0113	0.902	25.456
15.0	10	8	3.109	0.0571	0.969	18.636

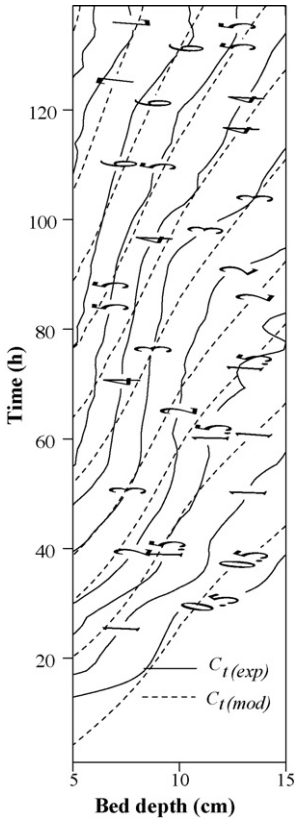

Fig. 5. Comparison of sorption contours of experimental effluent fluoride concentrations against theoretical values predicted by the Clerk's model at different bed depths (initial fluoride conc. = 8.65 mg l^{-1}, flow rate = 8 ml min^{-1}).

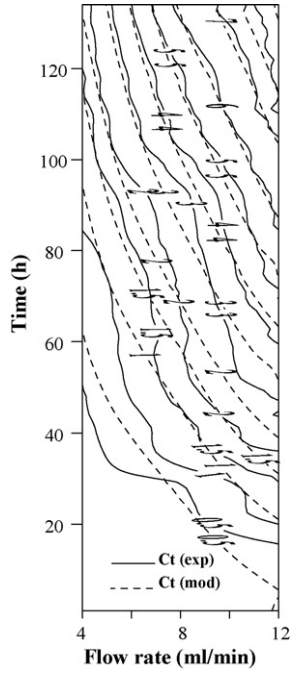

Fig. 6. Comparison of sorption contours of experimental effluent fluoride concentrations against theoretical values predicted by the Clerk's model at different flow rates (initial fluoride conc. = 8.65 mg l^{-1}, bed depth = 10 cm).

where

$$k_1 = \frac{N_0 K Z}{u} = \frac{k_{Th} q_{Th} M}{Q} = \tau k_{YN} \quad (10)$$

and

$$k_2 = K C_0 = k_{Th} C_0 = k_{YN} \quad (11)$$

It is obvious that only the characteristic parameters associated with these models varies but all the three models will predict essentially the same C_t/C_0 values for a particular data set, and are bound to give the same APE and R^2 values as illustrated in Table 3. But, the prominent and unique characteristic features of the respective models like service time (Hutchins BDST model), adsorption capacity (Thomas model) and time for 50% breakthrough (Yoon–Nelson model), enable further comparison. The APE values on service time, adsorption capacity and time for 50% breakthrough are 7.9952%, 6.199% and 11.64%, respectively. So, the predictions by Thomas model on its characteristic parameters turn more appropriate (as it renders the least error among the three) followed by Hutchins BDST model and Yoon–Nelson model. On comparing the R^2 and APE values of

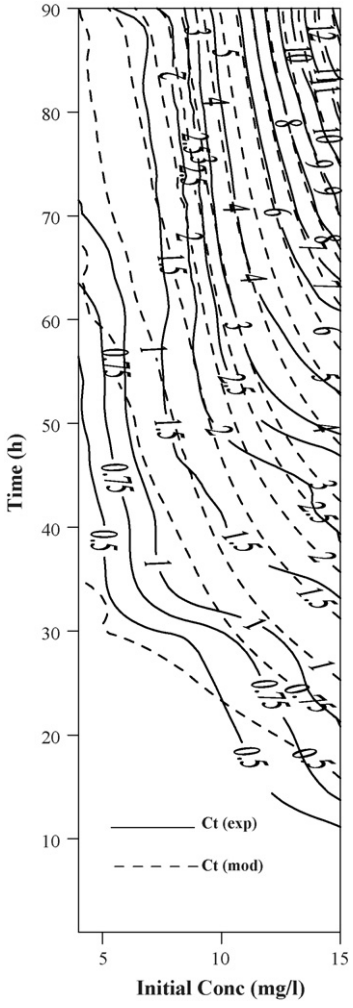

Fig. 7. Comparison of sorption contours of experimental effluent fluoride concentrations against theoretical values predicted by the Clerk's model at different initial fluoride concentrations (bed depth = 10 cm, flow rate = 8 ml min^{-1}).

Thomas model (Table 3) with that of the Clark's model (Table 4), it is seen that the latter correlates fairly better. So, though the Thomas model could fairly describe the sorption process, Clark's model is deemed to be the 'best fit' in terms R^2 and APE values.

Usually, the correlations between the experimental sorptive responses of the continuous flow fixed bed system with the best-fitting model, is represented by comparing their respective breakthrough curves (plotted against the same axial settings, usually C_t/C_0 versus t). But, a better comparison of the sorptive responses is possible through sorption contours (lines connecting same effluent fluoride concentration) as shown in Figs. 5–7. The sorption contours of the continuous flow system at different bed depths (Fig. 5), flow rates (Fig. 6), and initial fluoride concentrations (Fig. 7) provides a comparative assessment of the effluent fluoride concentrations of the treated water at any time, within the minimum ranges studied. Accordingly, it can be used as nomograms offering valuable inputs in the field implementation and process design by easily providing the service times of columns for desired effluent concentrations without further calculations and experimental run.

4. Conclusions

The batch study results confirm the feasibility of ALC in fluoride scavenging. The biphasic kinetic uptake marked by an initial rapid uptake followed by a slow removal may indicate the key role of mass transfer and prominence of surface bound sorption followed by diffusion. The batch sorption response of ALC is pointing to a complex removal process, occurring via multiple mechanisms. The column study results confirm its field applicability as it demonstrates reliable adsorption potential under different process conditions. The sorption profile of the adsorbent can be better described by Clark's model in the whole sorption ranges studied with consistent vigour than Thomas model. The sorption contours turns advantageous mainly because it provides a better visual comparison of the correlations between experimental and model data within the minimum time range of sorption studied. Also, the sorption contours directly provides the service times corresponding to any desired effluent fluoride concentrations without additional experimental run or using any parameter beforehand.

References

[1] UNDP, Human Development Report—Beyond Scarcity: Power, Poverty and the Global Water Crisis, United Nations Development Programme, 1 UN Plaza, New York 10017, USA, 2006.

[2] A.K. Susheela, A Treatise on Fluorosis, Fluorosis Research and Rural Development Foundation, New Delhi, India, 2003.

[3] C. Liang, R. Ji, S. Cao, Epidemiological analysis of endemic fluorosis in China, Environ. Carcinogenicity Ecotoxicological Rev. C 15 (2) (1997) 123–138.

[4] WHO, World Health Organization, New WHO Report Tackles Fluoride in Drinking-water, 2006 (http://www.who.int/mediacentre/news/new/2006/nw04/en/index.html).

[5] S. Ayoob, A.K. Gupta, Fluoride in drinking water: a review on the status and stress effects, Crit. Rev. Environ. Sci. Technol. 36 (2006) 433–487.

[6] J.R. Rao, T. Viraraghavan, Biosorption of phenol from a aqueous solution by *Aspergillus niger* biomass, Bioresour. Technol. 85 (2002) 165–171.

[7] Z. Aksu, F. Gönen, Biosorption of phenol by immobilized activated sludge in a continuous packed bed: prediction of breakthrough curves, Process Biochem. 39 (2004) 599–613.

[8] W.W. Choi, K.Y. Chen, The removal of fluoride from waters by adsorption, J. AWWA 71 (1979) 562–570.

[9] J.O. Hao, C.P. Huang, Adsorption characteristics of fluoride onto hydrous alumina, J. Environ. Eng. ASCE 112 (1986) 1054–1067.

[10] R.K. Daw, Experiences with domestic defluoridation in India, in: Proceedings of the 30th WEDC International Conference on People-Centred Approaches to Water and Environmental Sanitation, Vientiane, Lao PDR, 2004, pp. 467–473.

[11] D.C.K. Ko, J.F. Porter, G. McKay, Optimized correlations for the fixed bed adsorption of metal ions on bone char, Chem. Eng. Sci. 55 (2000) 5819–5829.

[12] Z. Zulfadhly, M.D. Mashitah, S. Bhatia, Heavy metals removal in fixed bed column by the macro fungus *Pycnoporus sanguineus*, Environ. Pollut. 112 (2001) 463–470.

[13] J.S. Noh, J.A. Schwarz, Estimation of the point of zero charge of simple oxides by mass titration, J. Colloid Interface Sci. 130 (1989) 157–164.

[14] R.A. Hutchins, New simplified design of activated carbon system, Am. J. Chem. Eng. 80 (1973) 133–138.

[15] H.C. Thomas, Heterogeneous ion exchange in a flowing system, J. Am. Chem. Soc. 66 (1944) 1664–1666.

[16] Y.H. Yoon, J.H. Nelson, Application of gas adsorption kinetics, Am. Ind. Hyg. Assoc. J. 45 (1984) 509–516.

[17] R.M. Clark, Evaluating the cost and performance of field-scale granular activated carbon systems, Environ. Sci. Technol. 21 (1987) 573–580.

[18] A.M. Raichur, J.M. Basu, Adsorption of fluoride onto mixed rare earth oxides, Sep. Purif. Technol. 24 (2001) 121–127.

[19] J.P. Chen, L. Wang, Characterization of metal adsorption kinetic properties in batch and fixed-bed reactors, Chemosphere 54 (2004) 397–404.

[20] W.J. Weber Jr., Physicochemical Processes for Water Quality Control, Wiley-Interscience Publication/John Wiley and Sons, New York, 1972.

[21] S. Ghorai, K.K. Pant, Equilibrium, kinetics and breakthrough studies for adsorption of fluoride on activated alumina, Sep. Purif. Technol. 42 (2005) 265–271.

[22] S.M. Maliyekkal, A.K. Sharma, L. Philip, Manganese-oxide-coated alumina: a promising sorbent for defluoridation of water, Water Res. 40 (2006) 3497–3506.

[23] W.J. Weber, J.C. Morris, Kinetics of adsorption on carbon from solution, J. Sanit. Eng. Div. ASCE 89 (1963) 31–39.

[24] K.G. Bhattacharyya, A. Sharma, *Azadirachta indica* leaf powder as an effective biosorbent for dyes: a case study with aqueous Congo Red solutions, J. Environ. Manage. 71 (2004) 217–229.

[25] A. Özcan, A.S. Özcan, Adsorption of Acid Red 57 from aqueous solutions onto surfactant-modified sepiolite, J. Hazard. Mater. 125 (2005) 252–259.

[26] I. Langmuir, The constitution and fundamental properties of solids and liquids, J. Am. Chem. Soc. 38 (1916) 2221–2295.

[27] H.M.F. Freundlich, Über die adsorption in lösungen, Z. Phys. Chem. 57 (1906) 385–470.

[28] L.D. Benefield, J.F. Judkins, B.L. Weand, Process Chemistry for Water and Wastewater Treatment, Prentice-Hall, Inc., Englewood Cliffs, NJ, 1982.